

1 Magma hybridisation and diffusive exchange recorded in heterogeneous
2 glasses from Soufrière Hills Volcano, Montserrat

3

4 Humphreys, M.C.S.^{1*}, Edmonds, M.^{1,2} Christopher, T.³ & Hards, V.⁴

5 ¹ Department of Earth Sciences, University of Cambridge, Downing Street, Cambridge, CB2 3EQ, UK

6 ² COMET+, National Centre for Earth Observation

7 ³ Montserrat Volcano Observatory, Flemmings, Montserrat, West Indies

8 ⁴ British Geological Survey, Keyworth, Nottingham, NG12 5GG

9

10 * Corresponding author: Tel: +44 (0)1223 333433; Email: mcsh2@cam.ac.uk

11

12 Running title: Magma hybridisation at Soufrière Hills Volcano

13

14

15

Special issue: Montserrat - CALIPSO

16

17

18

ABSTRACT

19 Arc volcanoes commonly show evidence of mixing between mafic and silicic magma.

20 Melt inclusions and matrix glasses in andesite erupted from Soufrière Hills Volcano

21 include an anomalously K₂O-rich population which shows close compositional

22 overlap with residual glass from mafic inclusions. We suggest that these glasses

23 represent the effects of physical mixing with mafic magma, either during ascent or by

24 diffusive exchange during the formation of mafic inclusions. Many glasses are

25 enriched only in K₂O, suggesting diffusive contamination by high-K mafic inclusion

26 glass; others are also enriched in TiO₂, suggesting physical mixing of remnant glass.

27 Some mafic inclusion glasses have lost K₂O. The preservation of this K-rich melt

28 component in the andesite suggests short timescales between mixing and ascent.

29 Diffusive timescales are consistent with independent petrological estimates of magma

30 ascent time.

31

32

INTRODUCTION

33 Many arc volcanoes are dominated by interaction between mafic and silicic magmas.

34 Recharge by hotter, more mafic material is frequently cited as an eruption trigger, and

35 transfer of volatiles may be important in both promoting mixing (e.g. *Eichelberger*,
36 1980) and advecting heat into, and remobilising, the overlying crystal-rich silicic
37 magma (*Bachmann and Bergantz*, 2006). Magma mingling (incomplete mixing)
38 produces quenched magmatic enclaves, crystal clusters and other clear disequilibrium
39 textures (*Anderson*, 1976; *Bacon*, 1986; *Clyne*, 1999). Recognising the products of
40 magma *hybridisation* (complete mixing) is important for understanding the relative
41 proportions and compositions of the end-member magmas, the likely impact of
42 repeated recharge, and the processes causing mass transfer between magmas.

43

44 Recent studies have shown that microlites of anomalously An-rich plagioclase (as
45 well as clinopyroxene and Mg-rich orthopyroxene) in intermediate arc magmas
46 originate in mafic magmatic enclaves or ‘mafic inclusions’ (*Martel et al.*, 2006;
47 *Humphreys et al.*, 2009a). The microlites are transferred into the andesite either
48 during mixing in the chamber (*Martel et al.* 2006) or by physical break-up and
49 disaggregation of mafic inclusions by shearing during ascent (*Humphreys et al.*,
50 2009a). This physical transfer of crystals will increase magma viscosity in the conduit
51 and therefore has implications for eruption dynamics, as well as the potential to be
52 used as a tracer of the mafic component. With effective mixing, one might also expect
53 to see a mafic melt component. Melt inclusions and matrix glasses are commonly
54 used to track magma evolution paths and assess magma storage conditions (e.g.
55 *Sisson and Layne*, 1993; *Wallace et al.*, 1995; *Blundy et al.*, 2006), so it is vital to
56 determine whether melt derived from the mafic magma is entering the andesite, and if
57 so, in what proportions and with what chemical signature. Quantifying the extent and
58 timescale of interaction between andesitic and mafic magma, which is thought to
59 drive the eruption, would also be invaluable for volcano monitoring and hazard
60 assessment. Here we examine evidence that magma mingling *does* involve transfer of
61 mafic-derived melt, preserved as heterogeneity in plagioclase-hosted melt inclusions
62 and matrix glasses.

63

64 **GEOLOGICAL BACKGROUND AND SAMPLES STUDIED**

65 The Soufrière Hills Volcano on Montserrat lies in the Lesser Antilles subduction zone
66 and has been active for approximately ~300 ka (*Harford et al.*, 2002). The most
67 recent eruption started in 1995, with a series of pulses of dome growth and explosive
68 activity, interrupted by long pauses when no magma was erupted. Major dome

69 collapses occurred in December 1997, July 1999, July 2001, July 2003 and May 2006.
70 Currently (September 2009) activity is limited to low-level residual activity, although
71 with continuing significant gas emissions (www.mvo.ms).

72

73 Products from the current eruption are porphyritic andesite, with phenocrysts of
74 hornblende, plagioclase, orthopyroxene and Fe-Ti oxides plus rhyolite glass or
75 groundmass. Disequilibrium crystal textures are common, including rare, resorbed
76 quartz phenocrysts, oscillatory zoning in plagioclase and hornblende, reversely zoned
77 orthopyroxene and sieve-textured plagioclase (*Murphy et al.*, 2000). The groundmass
78 contains microlites of plagioclase, orthopyroxene, clinopyroxene and Fe-Ti oxides as
79 well as rhyolitic glass, and may show extensive crystallisation, incipient
80 devitrification and deposits of cristobalite. Macroscopic mafic inclusions have been
81 described in detail (*Murphy et al.*, 1998; 2000) and contain plagioclase,
82 clinopyroxene, orthopyroxene, Fe-Ti oxides and rhyolitic interstitial glass; larger
83 inclusions also crystallise pargasitic amphibole (*Murphy et al.*, 1998). Many of the
84 microlites in the andesite are derived from mafic inclusions, as are crystal clusters, i.e.
85 mafic-derived fragments that can be recognised by texture and mineral compositions
86 (*Humphreys et al.*, 2009a).

87

88

RESULTS

89 We analysed plagioclase-hosted melt inclusions, matrix glass and residual mafic
90 inclusion glass from 23 samples erupted between July 2001 and July 2008 (see
91 supplementary table 1). Most of the samples represent typical andesite. Sample
92 MVO1532d is a heterogeneous mixture of nearly microlite-free rhyolite glass
93 containing euhedral quartz, plagioclase and hornblende, with fine-grained, crystal-rich
94 patches with very little remaining glass. Sample preparation and analytical methods,
95 together with the procedure used to correct for post-entrapment crystallisation (PEC)
96 of melt inclusions, are described in the auxiliary material.

97

Melt inclusions

99 Melt inclusions are rhyolitic, with 71-79 wt% SiO₂ (see supplementary data table 2;
100 figures show PEC-corrected values, normalised to 100% anhydrous). Compositions
101 are similar to those reported by *Edmonds et al.* (2001), *Harford et al.* (2003) and
102 *Buckley et al.* (2006). Two populations can be distinguished on the basis of K₂O

103 contents (figure 1). Most inclusions have 2–3 wt% K₂O, increasing with SiO₂ and Cl
104 contents, but a minority of inclusions has up to 6 wt% K₂O. For the low-K population,
105 Al₂O₃, CaO and Na₂O show a scattered negative relationship with SiO₂. FeO, MgO
106 and TiO₂ subtly increase with SiO₂, and also correlate with each other (e.g. figure 1d).
107 The high-K inclusion population has lower CaO than the low-K glasses, and slightly
108 lower Cl (figure 1). Two inclusions have high TiO₂ but low K₂O (figure 2). High-K
109 glasses were not present in pumiceous samples.

110

111 **Matrix glasses**

112 Matrix glass was analysed in samples without significant groundmass crystallisation
113 (supplementary table 1). Matrix glasses are rhyolitic, clustering at the SiO₂-rich end of
114 the melt inclusion trends (75-79 wt% SiO₂, figure 1). There are four groups of matrix
115 glasses: (i) high-K, low-Ti, (ii) low-K, low-Ti, (iii) high-K, high-Ti, and (iii) low-K,
116 high-Ti compositions (figure 2). High-K matrix glasses extend to lower CaO contents
117 than low-K glasses (figure 1b). Some glasses have anomalously low MgO. High-K
118 glasses were not present in the pumice samples.

119

120 **Mafic inclusion glass**

121 Residual mafic inclusion glasses are also rhyolitic (72-78 wt% SiO₂). In Si, Al, Fe and
122 Na composition they are indistinguishable from the melt inclusions. However, they
123 have distinctive high-Ti, high-K compositions (figure 2) and also show low CaO
124 contents, similar to the other high-K glasses. Many of the residual glasses also have
125 low MgO contents. Cl concentrations are variable but tend to be lower than in the
126 melt inclusions (figure 1).

127

128

DISCUSSION

129 In general, the negative correlations of Al₂O₃, CaO and Na₂O with SiO₂ in the melt
130 inclusions indicate decompression crystallisation dominated by plagioclase (e.g.
131 *Buckley et al.*, 2006). The positive correlation between FeO and MgO, and slight
132 increase of both MgO and FeO with SiO₂ suggests minor crystallisation of
133 orthopyroxene or hornblende as observed in the andesite. Ti-Fe variations are
134 consistent with crystallisation of minor Ti-magnetite. The low-K matrix glasses
135 follow mainly the same compositional trends as the low-K melt inclusions but tend
136 towards higher K₂O and higher SiO₂, as K is enriched in the melt during groundmass

137 crystallisation (*Harford et al.*, 2003). Low-K matrix glasses show decreasing MgO
138 with increasing SiO₂, consistent with groundmass crystallisation of orthopyroxene.
139 The trend of decreasing Cl with increasing K₂O in the matrix glass (figure 1f)
140 indicates degassing of Cl during decompression crystallisation (*Edmonds et al.*, 2001;
141 *Harford et al.*, 2003; *Humphreys et al.*, 2009b).

142 The low-Ca, low-Mg compositions of the mafic inclusion residual glasses are
143 consistent with significant crystallisation of clinopyroxene in the mafic inclusions.
144 The very high K₂O contents of mafic inclusion glasses are consistent with the lower
145 proportions of amphibole in the mafic inclusions and their lower bulk SiO₂ contents
146 relative to the andesite; their high TiO₂ may be related to the high TiO₂ of the bulk
147 mafic inclusions.

148

149 **Origin of high-K glass**

150 While the main compositional characteristics of the glass suite are consistent with
151 near-surface processes (see above), the K-rich signature of some glasses is not. The
152 occasional high TiO₂, high-K₂O, low MgO and low CaO contents are also seen in
153 previously reported matrix glasses (*Edmonds et al.*, 2001; 2002; *Harford et al.*, 2003;
154 *Buckley et al.*, 2006; see figure 1). These compositional features are largely shared by
155 the residual mafic inclusion glasses.

156 The anomalous glass compositions cannot be caused by boundary layer effects
157 during melt inclusion entrapment (*Baker*, 2008) because only slowly diffusing
158 incompatible elements should be enriched in the melt boundary layer, whereas K⁺
159 diffusivities are rapid (*Jambon*, 1983). Similarly, post-entrapment crystallisation of
160 host plagioclase should result in coupled increases of MgO, TiO₂ and K₂O with
161 decreasing CaO, which are not observed, and cannot account for anomalous matrix
162 glass compositions.

163 K-rich glasses or crystalline products have been ascribed to grain-boundary
164 partial melting of mafic cumulate nodules (*Dungan and Davidson*, 2004; *Heliker*,
165 1995) or assimilation of biotite-rich cumulates (*Reubi and Blundy*, 2008), with K-rich
166 and host melts mixing during subsequent nodule break-up. However, cumulate
167 nodules are relatively rare in Soufrière Hills andesite and were not observed in any of
168 the samples studied, while the high-K glasses are texturally indistinguishable from
169 ‘normal’ glasses and their host crystals are not obviously xenocrystic. Finally, K-rich

170 glasses are also found in mafic inclusions, which are widely agreed to form by rapid
171 quenching against a cooler host (*e.g. Wager and Bailey 1953; Yoder 1973*).
172 *Buckley et al. (2006)* ascribed the high-K compositions to hornblende
173 breakdown during slow magma ascent and mixing between more- and less-evolved
174 melts. Mass balance between the dissolving hornblende and the observed rims (cpx +
175 opx + plag + oxides) indicated that melts modified by hornblende breakdown should
176 thus be compositionally variable, with high TiO₂ and MgO but low SiO₂ and FeO.
177 The melts should all have high K₂O, Na₂O and Cl (*Buckley et al., 2006*). Neither of
178 their predicted trends fits with all the observed compositional variations (figure 1).
179 Interstitial melts in hornblende breakdown rims (*Buckley et al., 2006*) actually show
180 *both* high-K and low-K compositions (figure 1a), not just high-K compositions as
181 expected. We therefore conclude that decompression breakdown of hornblende cannot
182 adequately describe the high-K glasses.

183

184 **Magma hybridisation and diffusive contamination**

185 We propose that the K-rich melts are derived from, or affected by mixing with
186 intruding mafic magma. The K-rich compositions are similar to those of mafic
187 inclusion residual glass, and incorporation of K-rich melt into the host matrix is
188 consistent with transfer of microlites into the andesite groundmass by disaggregation
189 of mafic inclusions (*Humphreys et al., 2009a*). However, K₂O-TiO₂ concentrations
190 demonstrate the presence of four distinct glass compositions (see earlier; figure 2): (i)
191 low-K, low-Ti; (ii) low-K, high-Ti; (iii) high-K, high-Ti; and (iv) high-K, low-Ti.
192 This indicates that the mafic inclusion glasses are, for the most part, not being
193 transferred unmodified into the host andesite, and suggests diffusive modification.
194 Breaking open partially crystalline mafic inclusions would allow interaction between
195 host (rhyolite) melt from the andesite and residual rhyolite from the interior of the
196 mafic inclusions. Similarly, complete disaggregation of mafic inclusions would result
197 in physical transfer of K-rich, Ti-rich residual rhyolite, which can be modified by
198 diffusive re-equilibration with the host melt. Diffusion of TiO₂ is much slower than
199 that of K₂O (see later), so residual mafic glass that has lost K₂O by diffusion still
200 retains its high-Ti signature, whereas the high-K host rhyolite cannot gain TiO₂ by
201 diffusion (figure 2). The result is anomalously K-rich (but Ti-poor) host rhyolite melt,
202 and K-poor (but Ti-rich) residual mafic inclusion glasses. This process explains the
203 lack of ubiquitous Ti-enrichment of high-K melt inclusions and matrix glasses

204 compared with mafic inclusion glass. Once a pocket of K-rich melt is present in the
205 matrix of the andesite, it can be incorporated into melt inclusions by sealing of proto-
206 inclusions during ascent-driven crystallisation (see *Humphreys et al.*, 2008, figure 11).

207

208 **Timescales of between mixing and eruption**

209 The glass compositions and distribution can give further insight into the physical
210 processes involved in transfer of material. For example, the lack of K-rich glasses in
211 pumiceous samples (see earlier) implies that K-enrichment occurs during slow ascent.
212 Many of the K-rich compositions are matrix glass, with relatively few high-K melt
213 inclusions. This also suggests that transfer occurs primarily during low-pressure
214 ascent and crystallisation, and could be explained by lower shear stresses in the
215 conduit during rapid ascent of less viscous, less crystalline magma (e.g. *Melnik and*
216 *Sparks* 2005) compared with the highly viscous, strongly crystalline magma that
217 erupts slowly during dome growth.

218 Elemental diffusivities can be used to assess the timescales of this process
219 (*Sparks et al.* 1977; *Baker*, 1991). Alkali and alkaline earth diffusivities (D) in
220 anhydrous rhyolite are $D_{\text{Na}} \sim 1.6 \times 10^{-6} \text{ cm}^2/\text{s}$, $D_{\text{K}} \sim 8.9 \times 10^{-8} \text{ cm}^2/\text{s}$, and $D_{\text{Ca}} \sim 4.0 \times 10^{-10}$
221 cm^2/s at 900 °C (*Jambon* 1983). A first-order approximation of timescales (t) can
222 be made, ignoring the effects of possible differences in melt H₂O content, from $x \sim$
223 $2\sqrt{(Dt)}$, where x is the diffusion lengthscale, here taken to be 1 cm. Diffusive
224 timescales are 43 hours (Na⁺), 32 days (K⁺) and 20 years (Ca²⁺). In other words,
225 alkaline earth diffusion is slow relative to alkalis; diffusion of highly charged ions
226 (e.g. Ti⁴⁺) should be even slower than the alkaline earths (*Henderson et al.* 1985).
227 Diffusive contamination of alkalis should therefore be rapid, but modification of other
228 elements would be prohibitively slow (*Baker*, 1991). The K-enrichment of the
229 rhyolite matrix of the host andesite must therefore have occurred ~1 month or less
230 prior to eruption of the magma at the surface, in order to preserve the high-K
231 signature. This is consistent with timescales estimated by preservation of Fe-Ti oxide
232 zoning (*Devine et al.* 2003) and decompression breakdown rims on hornblende
233 (*Rutherford and Devine* 2003). The few high-Ti, low-K glasses, and the wide range of
234 K₂O contents of residual mafic inclusion glasses (figure 2) may reflect a spread to
235 longer timescales, allowing complete or partial re-equilibration of K₂O with the host
236 rhyolite. We also note that the K₂O contents of mafic inclusion and high-K host melts

237 are similar, whereas a diffusion couple should give slightly lower K_2O contents in the
238 host melt. There are two possible explanations for this: (i) the mafic inclusion glasses
239 are already diffused and their observed compositions are not primary, or (ii) the high
240 K_2O in the host rhyolite represents an uphill diffusion ‘spike’ similar to that observed
241 in experimental diffusion couples (*Bindeman and Davis 1999; van der Laan et al.*
242 *1994*). In either case, this observation reinforces the short timescales between mixing
243 and eruption.

244 The estimated diffusion timescales also suggest that Na_2O contents would
245 quickly be homogenised by diffusion between host andesite and mafic inclusions,
246 while original CaO contents should be preserved. We would also anticipate rapid
247 diffusion of volatiles (e.g. CO_2 and H_2O), particularly in more H_2O -rich melt (*Baker*
248 *et al. 2005*). It is difficult to assess the effects of mixing and diffusion on Ca and Na
249 as these elements are compatible in the crystallising assemblage and therefore
250 strongly affected by fractionation of plagioclase, whereas K is strongly incompatible.
251 However, the K-enriched glasses are slightly depleted in CaO relative to the normal
252 glasses, as is the mafic inclusion residual glass. The different diffusivities of CaO and
253 K_2O are not consistent with diffusive contamination of both elements: timescales long
254 enough for significant Ca diffusion would also eliminate any K_2O signature. The
255 lower CaO contents cannot be produced by crystallisation of quartz, or diffusion
256 gradients around growing plagioclase or pyroxene grains, as discussed earlier. We
257 suggest that the lower CaO might be related to continued crystallisation of
258 plagioclase.

259

260

CONCLUSIONS

261 Glass compositional heterogeneity from Soufrière Hills Volcano, Montserrat, is
262 interpreted as the result of mingling between hotter, mafic magma and the host
263 andesite. High- K_2O melt inclusions and matrix glasses in the andesite overlap with
264 the compositions of residual glass from mafic inclusions. However, K_2O and TiO_2
265 contents are decoupled: many high-K melt inclusions do not show high Ti as seen in
266 residual mafic inclusion glasses. This can be explained by diffusive exchange between
267 disaggregated mafic inclusion melt and host matrix melt. The host rhyolite gains K_2O
268 from mafic inclusions, but the original low TiO_2 contents are unchanged. Conversely,
269 high-Ti glasses with normal K_2O contents probably represent residual mafic inclusion
270 glass that has lost K_2O by diffusion. The preservation of such heterogeneity can be

271 used to estimate the timescales between mingling and magma ascent to the surface.
272 The timescales necessary to preserve K heterogeneity are on the order of a month,
273 which is consistent with magma ascent times estimated from hornblende breakdown
274 and Fe-Ti oxides.

275

276

ACKNOWLEDGEMENTS

277 MCSH acknowledges a Junior Research Fellowship from Trinity College, Cambridge.
278 ME acknowledges the NERC National Centre for Earth Observation (Theme 6:
279 Dynamic Earth) grant NE/F001487/1. VH publishes with the permission of the
280 Executive Director of the British Geological Survey (NERC). This work was partly
281 supported by the British Geological Survey. We thank Chiara Petrone for assistance
282 with electron microprobe analysis.

283

284

REFERENCES

285 Anderson, A.T. (1976). Magma mixing: Petrological process and volcanological tool.
286 *J Volcanol Geotherm Res* **1**, 3-33

287

288 Bachmann, O. & Bergantz, G.W. (2006). Gas percolation in upper-crustal silicic
289 mushes as a mechanism for upward heat advection and rejuvenation of near-solidus
290 magma bodies. *J Volcanol Geotherm Res* **149**, 85-102

291

292 Bacon, C.R. (1986). Magmatic inclusions in silicic and intermediate volcanic rocks.
293 *Journal of Geophysical Research* **91**, 6091-6112

294

295 Baker, D.R. (1991). Interdiffusion of hydrous dacitic and rhyolitic melts and the
296 efficacy of rhyolite contamination of dacitic enclaves. *Contrib Mineral Petrol* **106**,
297 462-473

298

299 Baker, D.R., Freda, C., Brooker, R.A. & Scarlato, P. (2005). Volatile diffusion in
300 silicate melts and its effects on melt inclusions. *Annals Geophys* **48**, 699-717

301

302 Baker, D.R. (2008). The fidelity of melt inclusions as records of melt composition.
303 *Contrib Mineral Petrol* **156**, 377-395

304

305 Bindeman, I.N. & Davis, A.M. (1999). Convection and redistribution of alkalis and
306 trace elements during the mingling of basaltic and rhyolite melts. *Petrology* **7**, 91-101

307

308 Blundy, J., Cashman, K & Humphreys, M. (2006). Magma heating by decompression-
309 driven crystallization beneath andesite volcanoes. *Nature* **443**, 76-80

310

311 Buckley, V.J.E., Sparks, R.S.J. & Wood, B.J. (2006). Hornblende dehydration
312 reactions during magma ascent at Soufrière Hills Volcano, Montserrat. *Contrib*
313 *Mineral Petrol* **151**, 121-140

314
315 Clynne, M.A. (1999). A complex magma mixing origin for rocks erupted in 1915,
316 Lassen Peak, California. *J Petrol* **40**, 105-132
317
318 Devine, J.D., Gardner, J.E., Brack, H.P., Layne, G.D. & Rutherford, M.J. (1995).
319 Comparison of microanalytical methods for estimating H₂O contents of silicic
320 volcanic glasses. *Amer Mineral* **80**, 319-328
321
322 Devine, J.D., Rutherford, M.J., Norton, G.E. & Young, S.R. (2003). Magma storage
323 region processes inferred from geochemistry of Fe-Ti oxides in andesitic magma,
324 Soufrière Hills Volcano, Montserrat, W.I.. *Journal of Petrology* **44**, 1375-1400
325
326 Dungan, M.A. & Davidson, J. (2004). Partial assimilative recycling of the mafic
327 plutonic roots of arc volcanoes: An example from the Chilean Andes. *Geology* **32**,
328 773-776
329
330 Edmonds, M.E., Pyle, D. & Oppenheimer, C. (2001). A model for degassing at the
331 Soufrière Hills Volcano, Montserrat, West Indies, based on geochemical data. *Earth*
332 *Plan Sci Lett* **186**, 159-173
333
334 Edmonds, M., Pyle, D. & Oppenheimer, C. (2002). HCl emissions at Soufrière Hills
335 Volcano, Montserrat, West Indies, during a second phase of dome building:
336 November 1999 to October 2000. *Bull Volcanol* **64**, 21-30
337
338 Eichelberger, J.C. (1980). Vesiculation of mafic magma during replenishment of
339 silicic magma reservoirs. *Nature* **288**, 446-450
340
341 Harford, C.L., Pringle, M.S., Sparks, R.S.J. & Young, S.R. (2002). *In* The Eruption of
342 the Soufrière Hills Volcano, Montserrat, from 1995 to 1999. T. H. Druitt, B. P.
343 Kokelaar, Eds. (Geological Society Memoir, London, 2002), vol. 21, pp. 93-113.
344
345 Harford, C.L., Sparks, R.S.J. & Fallick, A.E. (2003). Degassing at the Soufrière Hills
346 Volcano, Montserrat, recorded in matrix glass compositions. *J Petrol* **44**, 1503-1523
347
348 Heliker, C. (1995). Inclusions in Mount St. Helens dacite erupted from 1980 through
349 1983. *J Volcanol Geotherm Res* **66**, 115-135
350
351 Henderson, P., Nolan, J., Cunningham, G.C. & Lowry, R.K. (1985). Structural
352 controls and mechanisms of diffusion in natural silicate melts. *Contrib Mineral Petrol*
353 **89**, 263-272
354
355 Humphreys, M.C.S., Kearns, S.L. & Blundy, J.D. (2006). SIMS investigation of
356 electron-beam damage to hydrous, rhyolitic glasses: Implications for melt inclusion
357 analysis. *Amer Mineral* **91**, 667-679
358
359 Humphreys, M.C.S., Blundy, J.D. & Sparks, R.S.J. (2008). Shallow-level
360 decompression crystallisation and deep magma supply at Shiveluch Volcano. *Contrib*
361 *Mineral Petrol* **155**, 45-61
362

363 Humphreys, M.C.S., Christopher, T. & Hards, V. (2009a). Microlite transfer by
364 disaggregation of mafic inclusions following magma mixing at Soufrière Hills
365 volcano, Montserrat. *Contrib Mineral Petrol* **157**, 609-624
366

367 Humphreys, M.C.S., Edmonds, M., Christopher, T. & Hards, V. (2009b). Chlorine
368 variations in the magma of Soufrière Hills Volcano, Montserrat: Insights from Cl in
369 hornblende and melt inclusions. *Geochim Cosmochim Acta* **73**, 5693-5708
370

371 Jambon, A. (1983). Diffusion dans les silicates fondues: un bilan des connaissances
372 actualles. *Bull Mineral* **106**, 229-246
373

374 Martel, C., Radadi Ali, A., Poussineau, S., Gourgaud, A. & Pichavant, M. (2006).
375 Basalt-inherited microlites in silicic magmas: Evidence from Mount Pelée
376 (Martinique, French West Indies). *Geology* **34**, 905-908
377

378 Melnik, O. & Sparks, R.S.J. (2005). Controls on conduit magma flow dynamics
379 during lava dome building eruptions. *J Geophys Res* **110**, B02209
380

381 Murphy, M.D. , Sparks, R.S.J., Barclay, J., Carroll, M.R., Lejeune, A.-M., Brewer,
382 T.S., Macdonald, R., Black, S. & Young, S. (1998). The role of magma mixing in
383 triggering the current eruption of the Soufrière Hills volcano, Montserrat, West Indies.
384 *Geophys Res Letters* **25**, 3433-3436
385

386 Murphy, M.D., Sparks, R.S.J., Barclay, J., Carroll, M.R. & Brewer, T.S. (2000).
387 Remobilization of andesite magma by intrusion of mafic magma at the Soufrière Hills
388 Volcano, Montserrat, West Indies. *J Petrol* **41**, 21-42
389

390 Reubi, O. & Blundy, J. (2008). Assimilation of plutonic roots, formation of high-K
391 'exotic' melt inclusions and genesis of andesitic magmas at Volcano de Colima,
392 Mexico. *J Petrol* **49**, 2221-2243
393

394 Rutherford, M.J. & Devine, J.D. (2003). Magmatic conditions and magma ascent as
395 indicated by hornblende phase equilibria and reactions in the 1995-2002 Soufrière
396 Hills magma. *J Petrol* **44**, 1433-1454
397

398 Saito, G., Uto, L., Kazahaya, KK., Shinohara, H., Kawanabe, Y. & Satoh, H. (2005).
399 Petrological characteristics and volatile content of magma from the 2000 eruption of
400 Miyakejima Volcano, Japan. *Bull Volcanol* **67**, 268-280
401

402 Sisson, T.W. & Layne, G.D. (1993). H₂O in basalt and basaltic andesite glass
403 inclusions from four subduction-related volcanoes. *Earth Plan Sci Letts* **117**, 619-635
404

405 Sparks, R.S.J., Sigurdsson, H. & Wilson, L. (1977). Magma mixing: a mechanism for
406 triggering acid explosive eruptions. *Nature* **267**, 315-318
407

408 Van der Laan, S., Zhang, Y., Kennedy, A.K. & Wyllie, P.J. (1994). Comparison of
409 element and isotope diffusion of K and Ca in multicomponent silicate melts. *Earth
410 Plan Sci Letts* **123**, 155-166
411

412 Wager, L.R. & Bailey, E.B. (1953). Basic magma chilled against acid magma. *Nature*
413 **172**, 68-69
414
415 Wallace, P.J., Anderson, A.T. & Davis, A.M. (1995). Quantification of pre-eruptive
416 exsolved gas contents in silicic magmas. *Nature* **377**, 612-616
417
418 Yoder, H.S. (1973). Contemporaneous basaltic and rhyolitic magmas. *Amer Mineral*
419 **58**, 153-171
420

421 **Figures**

422 Figure 1

423 Compositions of melt inclusions, matrix glasses and mafic inclusion residual glasses.
424 Melt inclusions (diamonds) and matrix glasses (circles) are divided into high-K (open
425 symbols) and low-K (filled symbols) compositions. Crosses represent mafic inclusion
426 glasses. Grey symbols represent previously published glasses from Soufrière Hills
427 (pluses, *Edmonds et al.*, 2001, 2002; squares, *Harford et al.*, 2003; triangles, *Buckley*
428 *et al.*, 2006). Grey dashes: glasses in hornblende breakdown rims (*Buckley et al.*,
429 2006). Large arrows indicate the schematic effects of hornblende breakdown reactions
430 (reactions 2 and 3, *Buckley et al.*, 2006), or the effect of 5% post-entrapment
431 crystallisation of plagioclase (pl).

432

433 Figure 2

434 Decoupled compositional variations in K₂O and TiO₂ for all glasses. Thick grey
435 arrows indicate how diffusive contamination of K₂O affects melt compositions. TiO₂
436 is unaffected because of its very low diffusivity. Symbols as for figure 1.

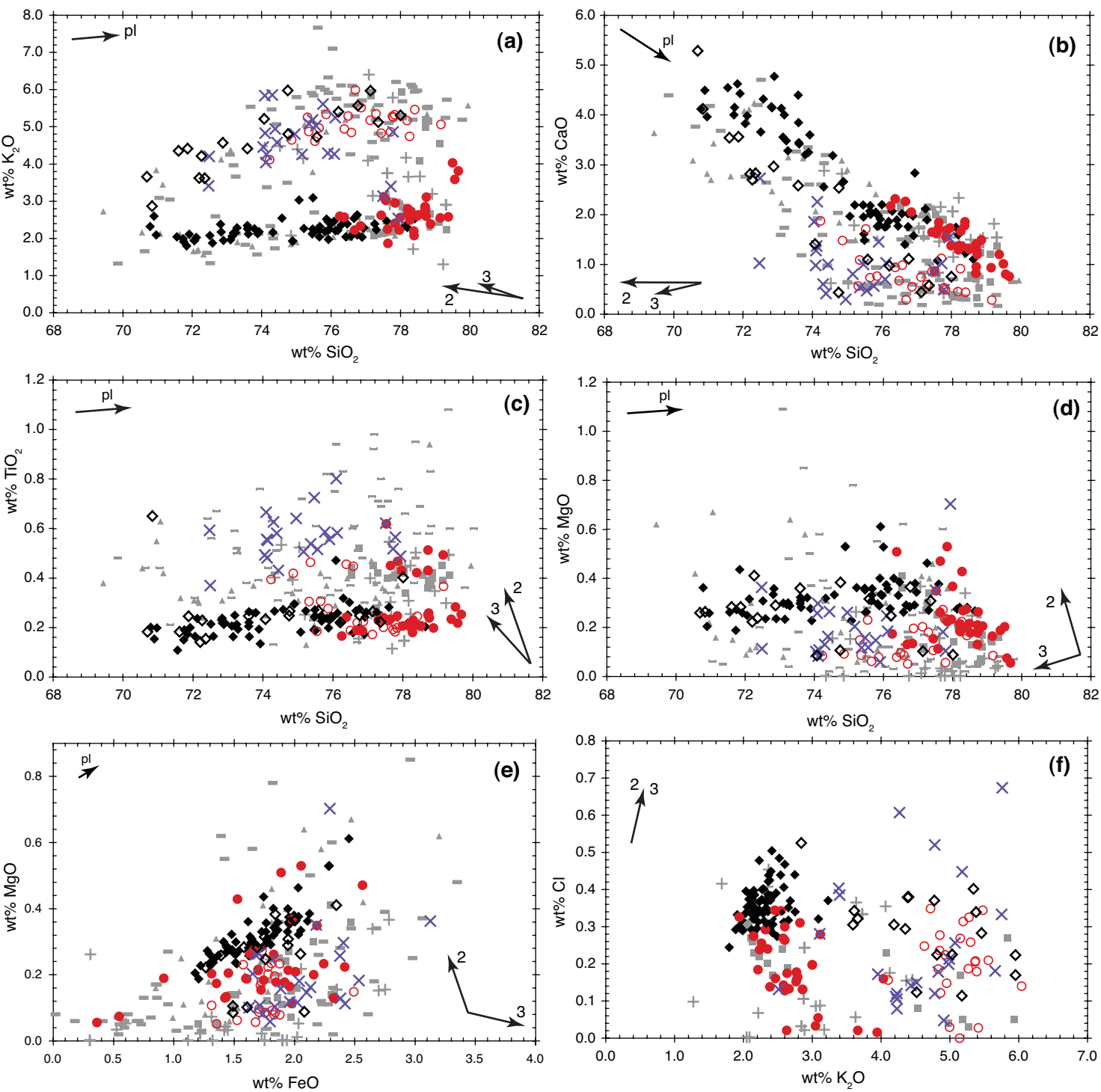


Figure 1

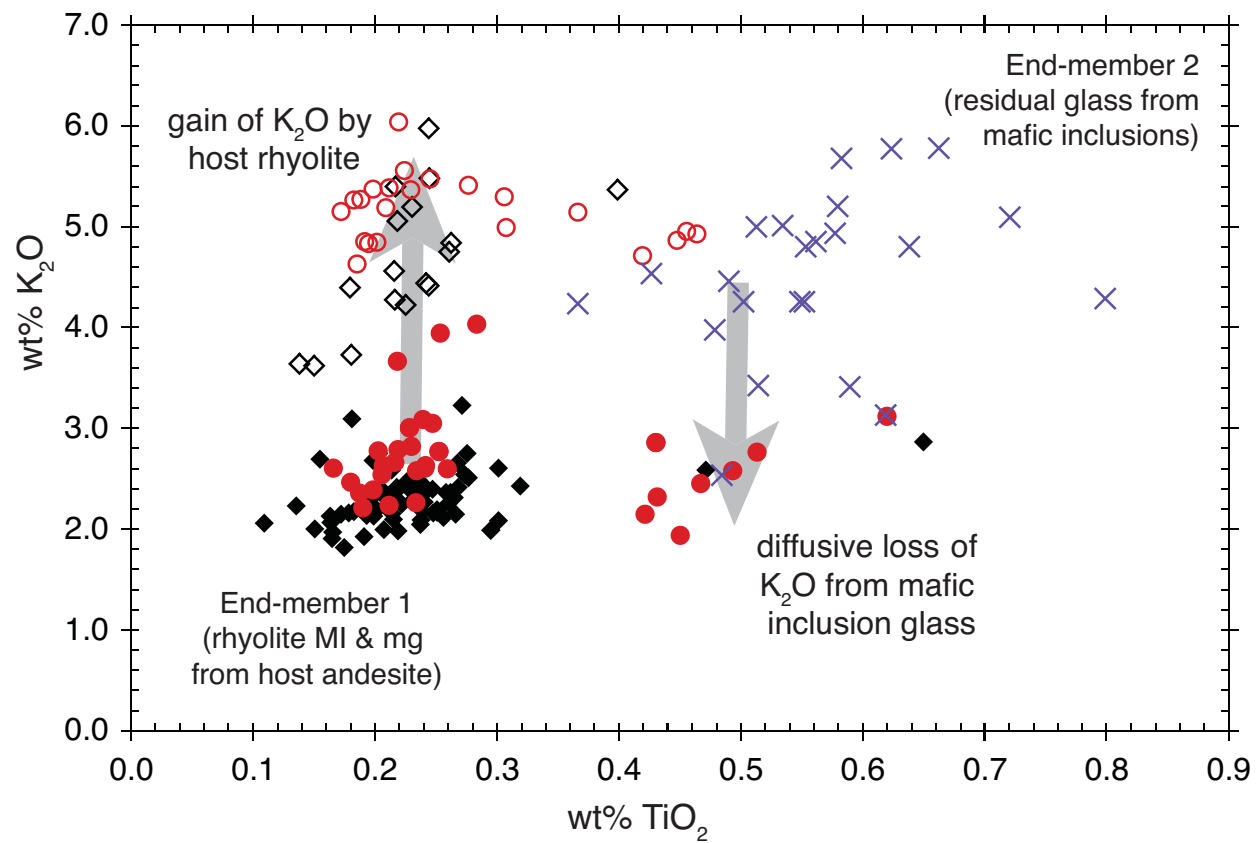


Figure 2